Chapter 3

Optimal Design of Brushless Doubly Fed Reluctance Machine

Mandar Bhawalkar, Gopalakrishnan Narayan and Yogesh Nerkar

Additional information is available at the end of the chapter

http://dx.doi.org/10.5772/intechopen.74805

Abstract

Optimization techniques are widely used in the design of electrical machines to obtain maximum performance at minimal capital cost. After a brief overview of some of the optimization techniques employed in electrical machine design, this chapter highlights the features of brushless doubly fed reluctance machine (BDFRM) and its optimal design. The simple and robust construction, variable speed operation, better performance compared to traditional counterpart, and requirement of partially rated converter for speed control have made BDFRM an attractive alternative for variable speed applications such as pumps, blower, and wind generators. Due to unusual construction of BDFRM, conventional design procedures cannot be applied. A few critical issues in the design of BDFRM that greatly affect its performance are discussed. Design optimization is performed using nonlinear programming technique for 6-4-2 pole reluctance rotor and 8-6-4 pole ducted rotor configurations of BDFRM. 2 kW prototypes are then constructed for laboratory use. The performance of the prototypes is examined through finite element analysis (FEA) employing Maxwell 16 software. The test results are also presented.

Keywords: optimization, nonlinear programming, objective function, BDFRM, optimal design of BDFRM, finite element analysis

1. Introduction

Many industrial applications demand efficient, robust, and cost-effective variable speed drives. Brushless doubly fed reluctance machine (BDFRM) is one of the better alternatives for induction motors due to simple and rugged construction, higher efficiency, absence of rotor winding, slip rings and brushes, and reduced maintenance cost. Last but not least, a partially

rated converter is sufficient for control of speed in either direction of rated speed [1, 2]. These benefits are useful to BDFRM in generator mode in wind power applications.

The fierce competition in world market, increasing cost of energy supplies, and regulations for conservation of energy and resources are the key forces for design optimization of electrical machines. Electrical machine design is a complex process which can be realized as articulation or formulation subjected to restrictions imposed by various factors such as nonlinear characteristic of different material compositions, performance parameters, etc. and ability to achieve acceptable performance. The expected outcome of optimization is to minimize the capital and running costs and increased service life [3, 4]. The optimization is aimed at getting desirable solution of objective function(s) to maximize performance subjected to constraints. The design by analysis is based on estimation of performance of a machine from known variables and their inter-dependability. The known variables are usually design specifications or system parameters. In the design, the desired performance parameters are substituted in realistic mathematical model of machine which is then solved iteratively. However, the range of acceptable solutions may not necessarily yield optimum results with respect to cost, material requirements, and other factors, and hence machine design problem is linked to optimization and needs to be solved iteratively.

The organization of this chapter is as follows: Section 2 presents an overview of optimization techniques, and Section 3 gives a brief introduction to BDFRM to develop better understanding of machine. Section 4 discusses design considerations of BDFRM. An objective function is developed to minimize the active material requirements. Nonlinear programming is carried out for the optimal design of BDFRM. Section 5 presents the development of 2 kW prototypes. Section 6 discusses simulation results using Maxwell 16 (finite element software). This followed by test results of prototypes in Section 7. Section 8 presents conclusions.

2. Overview of optimization techniques

The optimization problems can be classified [5] as shown in **Table 1**. The classification of optimization problem depends on the nature of problem, operational constraints, and design limitations. The selection of algorithm for solving optimal problem depends not only on the types of objective function used but also on how its first and second derivatives are computed.

The optimization methods can be further classified broadly as classical methods and recent or advanced methods. The classical methods use continuous and differentiable functions [5], and these methods include single variable and multivariable optimization with and without constraints. Depending on the nature of objective function and design variables, optimization problem can be linear or nonlinear optimization with or without constraints. There is an inexhaustive list of different optimization techniques used for different applications looking into the aspects of various design/operational/environmental constraints. These methods are

Based on	Classification
Existence of constraints	Unconstrained/constrained optimization
Nature of design variables	Static/dynamic/trajectory optimization
Physical structure of problem	Optimal/nonoptimal control
Equations involved and objective function	Linear/nonlinear/geometric/quadratic programming
Permissible values of the design variables	Integer programming/real-valued programming
Nature of variables	Deterministic/stochastic programming
Separable functions	Separable/non-separable programming
Number of objective functions	Single objective/multiobjective programming

Table 1. Classification of optimization problems.

Optimization	Optimization methods
Classical	Single variable, multivariable with or without constraints
LP	Simplex, revised simplex, dual simplex method
One-dimensional nonlinear programing (NLP)	Elimination methods—unrestricted search, exhaustive search, dichotomous search, Fibonacci method, golden section search Interpolation methods—quadratic interpolation, cubic interpolation Direct root methods—Newton, quasi-Newton, and Secant
NLP with no constraint	Direct search—random search, grid search, univariate, pattern search, Powell, Hooke-Jeeves, Rosenbrock, and simplex Descent methods—steepest descent, Fletcher-Reeves, Newton, Marquardt, quasi-Newton, Davidon-Fletcher-Powell, and Broyden-Fletcher-Goldfarb-Shanno
Constrained NLP	Direct methods—random search, heuristic search, complex, objective and constraint approximation, sequential linear programming, sequential quadratic programming, method of feasible directions, Zoutendijk, Rosen's gradient projection, generalized reduced gradient Indirect methods—transformation of variables, sequential unconstrained minimization, interior penalty, exterior penalty, and augmented Lagrange multiplier
Advanced optimization methods	Geometric programming, dynamic programming, integer programming, stochastic programming, simulated annealing method, genetic algorithm, artificial neural network, fuzzy system, particle swarm optimization, differential algorithm, filled function method, evolutionary algorithms, design of experiments—central composite design, Latin hypercube design

Table 2. Different optimization techniques.

given in **Table 2** [3–9]. Classical optimization methods are found wanting due to increasing complexities, inter-dependability of design variables, and constraint functions. Therefore, nonlinear optimization methods with constraints are widely used along with newer methods such as genetic algorithms, artificial neural networks, and fuzzy logic techniques.

In the optimal design of electrical machines, the model of problem to be solved is to be selected along with choice of algorithms, variables, constraint functions, and objective functions. The classical methods such as random search method, simplex method, Hooke and Jeeves method, Powell and David-Fletcher-Powell method, and penalty function methods have been used in earlier decades. Most of them are nonlinear programing types as nonlinearities are imposed due to materials, operational issues, etc. Mathematically, these problems can be stated as.

$$minimize\, f(X) \tag{1}$$

$$subjected\ to\ g(X) \geq 0 \tag{2}$$

where X is an n-dimensional vector, f(X) is an objective function, and g(X) represents design constraints. The bounded region enclosed by g(X) = 0 where X is feasible.

The multiobjective function optimization problems are more complex as the feasible solutions are conflicting and practically impossible to obtain optimal solution to all objective functions simultaneously. Hence, a set solutions providing tradeoff between objective functions are acceptable.

The recent methods such as differential evolutions (DE), genetic algorithms (GA), evolutionary algorithms (EA), and particle swarm optimization (PSO) are used in machine design optimization [7–9]. These methods use a set of populations as initial approximation unlike classical method and are stochastic in nature. As these methods can optimize nonlinear functions containing continuous and discrete variables, they are the most suited ones for machine design problems. A recent study [7] has shown that DE may not be always the fastest, but produces the best results. GA is based on principles of natural genetics and natural selection. It encodes parameters as bit string, and then manipulation is performed using logical operators [10]. Another technique design of experiments (DoE) is a statistical method that effectively quantifies the effect of changes in design variables or machine response. This method includes one factor at a time and is suitable for a limited number of variables. Hence, advanced DoE methods such as central composite design (CCD) and Latin hypercube design (LHD) are used [7]. EA encodes parameters as floating point arithmetic operators. These methods are usually linked to finite element analysis solvers to optimize the machine design. PSO is also gaining importance in electrical machine design as it is used to get appropriate fitness evaluation function, which represents the relationship between design variables and machine response. In PSO the potential solution (particles) flies through the problem space by following the current optimum particles after initialization with random particles. In addition ANN and fuzzy logic are also gaining wide-scale acceptance. ANN is used due its immense computational powers. Appropriate selection of network topology and layers is very important. This method also needs voluminous data for training neural networks. ANN can be trained to learn the relationship between input and output parameters of electrical machines [11]. Fuzzy logic is also being tried out for electrical machine design [12]. The fuzzy sets are formed from decision and controlled variables. A qualitative approach is used for deriving membership and objective functions. A combination of stochastic method such as such as neuro-fuzzy, fuzzy, and genetic algorithm is also used in optimization [13].

http://dx.doi.org/10.5772/intechopen.74805

3. Brushless doubly fed reluctance machine (BDFRM)

A BDFRM consists of two sets of three-phase sinusoidally distributed windings with 2p and 2q poles ($p \neq q$) embedded in the same slots of stator. The rotor has no winding. However, the number of poles on rotor and stator is given by Eq. (3):

$$P_r = (p + q) \tag{3}$$

The schematic representation of BDFRM is shown in **Figure 1**. One of the two windings on stator is called as power/main winding, and the other is known as control/secondary winding. There is no direct magnetic coupling between two windings [1, 2]. The interaction between two windings takes place through rotor only. The power winding is directly excited by grid having frequency 50/60 Hz. The main role of power winding is to set up a magnetic field in the machine and deals with power exchange with grid. The control winding is excited by variable frequency, variable voltage obtained from a power electronic converter, or any other dedicated source. This winding controls torque developed and operating speed of the BDFRM. When two windings are excited, the MMFs are set up along the air gap. The MMFs F_p and F_c are the functions of rotor position where F_p and F_c are MMFS of power and control winding, respectively.

The interaction of two MMFs produces resultant air gap flux density and is responsible for development of electromagnetic torque which can be obtained analytically assuming infinite permeability of magnetic circuit, uniformly distributed windings, sinusoidal currents through windings, and representation of air gap by sine function.

The MMFs produced by these two windings are given by Eqs. (4) and (5), and the spatial distribution of power winding and control winding MMFs is shown in **Figure 2**:

$$F_p(\theta_{mg}) = F_{mp} \cos\left(\omega_p t - p\theta_{mg} + \varphi_p\right) \tag{4}$$

$$F_c(\theta_{mg}) = F_{mc} \cos\left(\omega_c t - q\theta_{mg} + \varphi_c - \alpha\right) \tag{5}$$

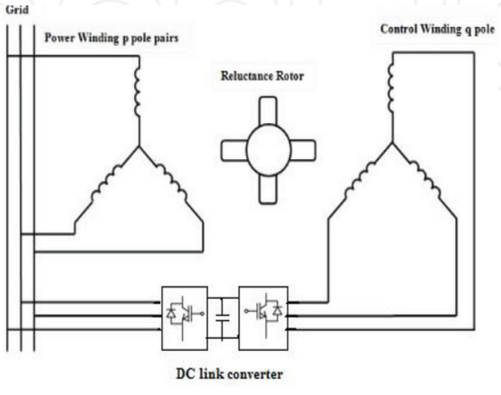

Figure 1. Schematic representation of BDFRM.

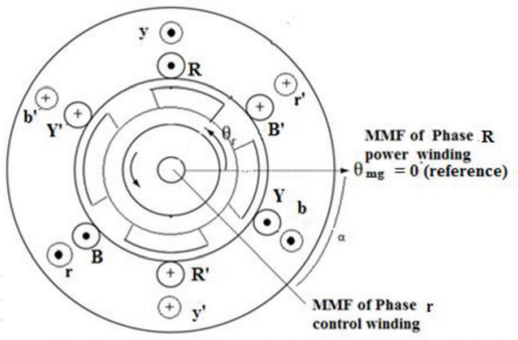

Figure 2. MMFs of power and control windings.

The resultant MMF acting along the air gap in BDFRM is the sum of MMFs produced by power and control windings. The interaction of two MMFs through rotor results in modulation of flux densities of both windings. These flux densities have fundamental frequency component along with two sidebands. Or, it can be interpreted that sinusoidal MMFs produced by two windings get modulated into a fundamental and two sidebands through inverse air gap function. The modulated frequency components are also time dependent and have spatial coordinates. Further, the coupling between two windings is decided by the pole numbers and sideband frequency component. The condition for torque production is that there is coupling between sidebands of one of the windings with fundamental frequency component of other windings. One of the sideband frequencies of power winding linking with fundamental frequency of control winding is given by Eq. (6):

$$\omega_m = \left(\omega_p + \omega_c\right)/P_r \tag{6}$$

The space phasor voltage equations of BDFRM are used to get electromagnetic torque T_e developed which is given by Eq. (7):

$$T_e = (3/2)(p+q)\left(\psi_{dc} i_{qc} - \psi_{qc} i_{dc}\right) \tag{7}$$

Three distinct modes of operations are possible depending upon the frequency of control winding:

1. If $\omega_c = 0$, control winding excitation is dc, and the machine operates as a conventional synchronous machine.
2. If $\omega_c > 0$, this results in super synchronous operation. The phase sequence of power winding is same as that of control winding.
3. If $\omega_c < 0$, this results in sub-synchronous operation. The phase sequence of power winding is different from that of control winding.

BDFRM is therefore potentially useful as a variable speed drive.

4. Design considerations in BDFRM

The reluctance machine has higher leakage inductances which lead to poor operational power factor. Incorporation of advanced rotors that orient flux in the preferred direction can improve the power factor [2, 14]. The other issues are smaller torque density and larger torque pulsation which can be improved by a careful design of BDFRM with higher saliency ratio. There are several considerations in design of BDFRM; the main issues are highlighted below [15, 16]:

1. What is the basis of selection of specific electric and magnetic loadings and stator slots?
2. What are the criteria for the choice of the number of poles in stator and on rotor?
3. Should there be two independent windings wound for different poles or one winding wound for different poles in stator?
4. Do the stator windings have to be full pitched or short pitched?
5. Which of the two windings should be selected as power winding/control winding?
6. What will be the practical range of control winding frequency and control winding voltage?
7. Should the choice of air gap length based on magnetic pull or any other factor?
8. Is there any possibility of reduction of space harmonics, noise, losses in stator windings, and rotor core?
9. How to reduce or mitigate bearing currents due to PWM inverters and unbalanced magnetic pull?

The selection of specific loadings depends on permissible losses, overload capacity, magnetic saturation, forces acting on rotor surface, etc. Selection of the number of stator slots and rotor ducts is very important in elimination of space harmonics in resultant MMF waveform. As the resultant MMF wave along the air gap is superposition of two MMFs, it has large space harmonics. **Table 3** gives suitable combinations of stator slots and rotor ducts.

Proper selection of the number of poles on stator and rotor decides the magnetic coupling between stator and rotor which governs the torque production. The higher the coupling coefficient, the higher the torque production. This can be inferred from **Figure 3**.

S. no.	Stator slots	Rotor ducts	Lower-order space harmonics	
			h_{sp}	h_{sq}
1	48	54	104	104
2	48	60	52	56
3	48	66	136	140
4	48	72	136	140

Table 3. Minimum number of space harmonics for same stator and rotor slots [17, 18].

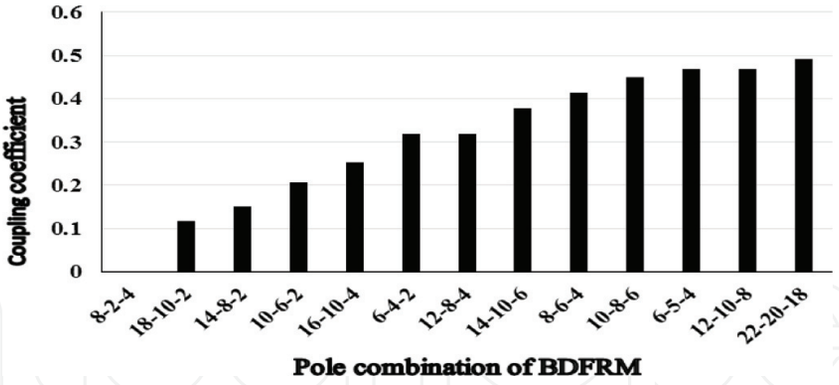

Figure 3. Coupling coefficient vs. pole combinations of BDFRM.

The selection of two or single winding in the stator is done on the basis of relative merits of both cases. Though it is costly, provision of two independent windings is more convenient for construction and control. With two independent windings, there is a great flexibility in winding pitches, and short pitching can be used to minimize the effect of space harmonics. The higher pole winding is generally considered as power winding [15] though there is no definite rule. There is no clarity over the voltage rating of control winding. It can be understood that in V/f control mode voltage will vary as frequency to avoid saturation in magnetic circuit. Is V_c/f_c equal to V_p/f_p? Or, can it be different? The length of air gap greatly affects the performance of the machine as MMF requirement increases with the length of air gap. Hence, selection of air gap needs a compromise.

Design of BDFRM is a complex process and involves various aspects of electromagnetism, thermal engineering, and machine design. The thermal and mechanical engineering aspects are similar to conventional machine design criteria. In BDFRM mechanical geometries differ from conventional machines, and hence conventional design procedures may have to be modified suitably. Therefore, analytical design approach is used. The voltage and current ratings of BDFRM decide the capacity of power electronic converter. The major consideration is the cost of machine which depends on the volume of active material used. For continuous operation the torque should be present over the designed range of speed, and the losses in BDFRM should be kept minimum for restricting temperature rise.

4.1. Steps in the design of BDFRM

For the design of BDFRM rating of the machine (2 kW), a number of pole configurations on stator and rotor (8-6-4), rated synchronous speed (500 rpm), rotor construction (ducted), etc. are specified. With these inputs the design of the machine can be carried out on the guidelines suggested in [15, 16, 19]. After deciding the rating and the input data of BDFRM, the steps involved in the design are shown as a flow graph in **Figure 4**. Two configurations of BDFRM are short listed for prototype development: 6-4-2 with reluctance rotor, and the other one is 8-6-4 circular ducted rotor. Initial values of flux density (0.5 T), current density (4 A/mm^2), integral slot, and full-pitched windings are assumed. A nonlinear programing (NLP) method is selected for design optimization of BDFRM as nonlinearities of materials and magnetic circuit have to be taken into considerations.

http://dx.doi.org/10.5772/intechopen.74805

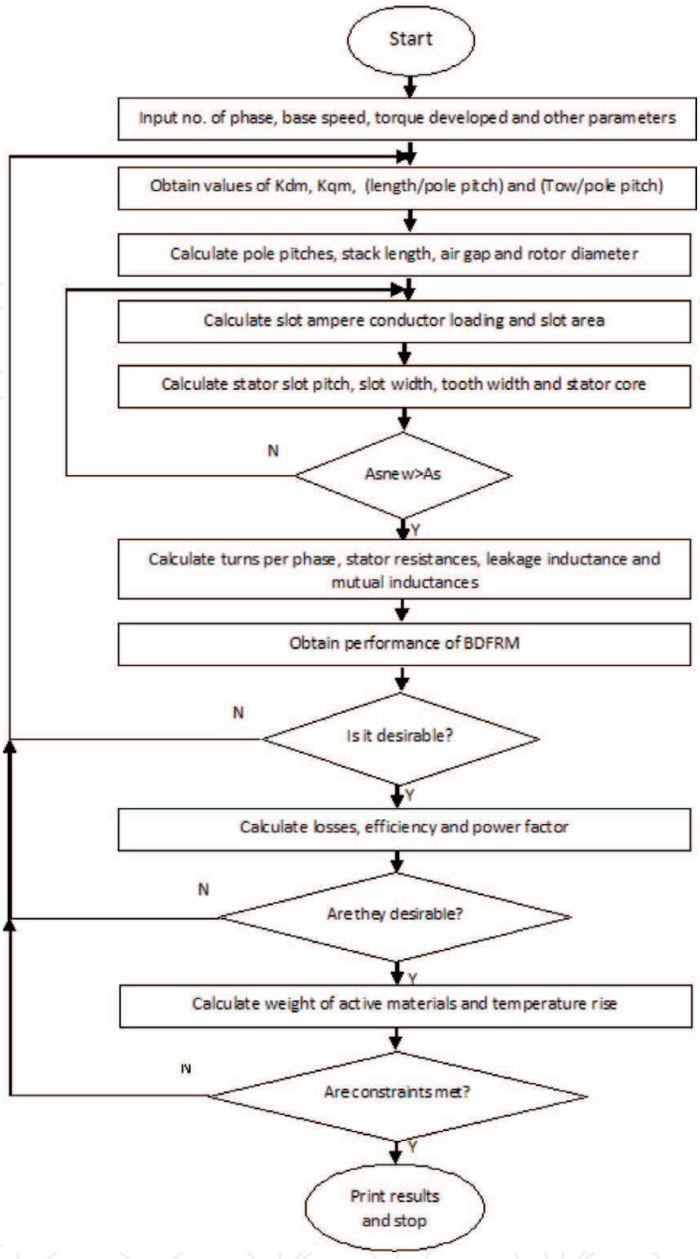

Figure 4. Flow graph for design optimization.

4.2. Objective function

A NLP problem involves the selection of independent variables, the development of objective function, and the constraint function for design of electrical machine. The objective function can be the cost of active materials or overall weight of machine or performance parameters, etc. The performance parameters of a machine can be used as constraints, e.g., pullout torque/full-load power factor/slot space factor/specific loadings/maximum flux density in stator tooth/temperature rise/shaft diameter. While designing BDFRM only a few variables are considered as independent, and these are given below [6, 19]:

1. Stator bore radius (x_1)
2. Gross length of stator stack (x_2)

3. Width of stator slot (x_3)
4. Depth of stator slot (x_4)
5. Cross section of winding conductors (x_5)
6. Depth of stator core (x_6)
7. Minimum length of air gap (x_7)
8. Maximum length of air gap (x_8)
9. Number of turns per pole per phase (x_9)
10. Number of slots in stator (x_{10})

The variables such as height of tooth lip, slot wedge thickness, slot opening, etc. have little effect on the overall performance. They are assumed to be known and constant and hence not considered in the optimization. The variables considered in BDFRM design are shown in **Figure 5**.

The constraint function limits considered in the design of BDFRM are:

1. Maximum torque ≥ 1.5 time full-load torque
2. Full-load power factor ≥ 0.5 lagging
3. Current density ≤ 4.5 A/mm^2
4. Slot fill factor ≤ 65%
5. Maximum tooth flux density ≤ 2 T
6. Maximum flux density in stator core and yoke ≤ 1.3 T
7. Specific electrical loading ≤ 25,000 ampere-conductor/m
8. Width of stator slot ≥ 6 mm

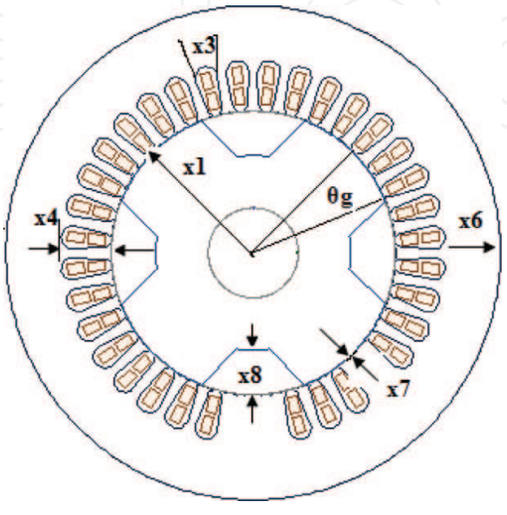

Figure 5. Illustration of the design variables of BDFRM.

9. Temperature rise ≤ 50°C

10. Shaft diameter ≥ 25 mm

The objective function [20] for reluctance rotor configuration is derived as given below.

The outer radius of stator (S_r) lamination is given by Eq. (8):

$$S_r = (x_1 + x_4 + x_6) \tag{8}$$

The volume of stator laminations is calculated by Eq. (9):

$$V_{is} = L_i \left[\pi(x_1 + x_4 + x_6)^2 - \pi {x_1}^2 - x_3\, x_4 x_{10}\right] \tag{9}$$

where $L_i = 0.9(x_2 - n_d b_d)$.

Thereafter, volume of rotor is calculated by using Eq. (10):

$$V_{ir} = 0.9x_2\ \left(\pi {x_1}^2 - 4{x_1}^2\ \left(\theta_g - sin\theta_g\ cos\theta_g\right)\right) \tag{10}$$

Approximate mean length of turns for power and control windings are given by Eqs. (11) and (12), respectively:

$$L_{mtp} = 2x_2 + 2.3\pi(x_1/p) + 0.152 \tag{11}$$

$$L_{mtc} = 2x_2 + 2.3\pi(x_1/q) + 0.152 \tag{12}$$

The volume of the copper required for power and control windings is given by Eq. (13):

$$V_c = 2\left(pmx5.x9.L_{mtp} + qmx_5 x_9 L_{mtc}\right) \tag{13}$$

Finally, the objective function is obtained as in Eq. (14) taking into account of the weights of active materials:

$$F = D_i(V_{is} + V_{ir}) + D_c V_c \tag{14}$$

For ducted rotor BDFRM, rotor iron volume is derived as given by Eq. (15):

$$V_{ir} = 0.9x_2\ \left(\pi {x_1}^2 - \pi\ {d_{sh}}^2\right) - 6(A_1 + A_2 + A_3 + A_4 + A_5 + A_6) \tag{15}$$

where A_1–A_6 represent duct areas and are calculated on the basis of width of the duct and angular distribution over a rotor pole.

Eq. (15) is substituted in place of V_{ir} in Eq. (14) to get the objective function for ducted rotor BDFRM.

The specifications of two 2 kW BDFRM configurations are given below:

a. Power winding poles—6, control winding poles—2, rotor poles(reluctance)—4, rated speed 750 rpm, stator slots 36 with single winding in stator

Sr.	Description	Initial values	Optimized 6-4-2 BDFRM
1	Stator outer diameter	204 mm	165 mm
2	Stator internal diameter (stator bore)	113.29 mm	91 mm
3	Length of air gap (main)	0.45 mm	0.5 mm
4	Rotor external diameter	112 mm	90 mm
5	Effective axial length of machine	95	80 mm
6	Stator yoke length	17 mm	15.3 mm
7	Rotor inner diameter	40 mm	50 mm
8	Conductor area for both windings	0.665 mm^2	0.663 mm^2
9	Depth of stator slot	21.9 mm	18.016 mm
10	Stator tooth width	3 mm	4 mm
11	Slot area	79.79 mm^2	69.25 mm^2
12	Total slot space factor	0.45	0.45
13	(ac) Loading of power/control winding	5000 A/m	5140 A/m
14	Max flux density in stator tooth	1.46 T	1.3 T
15	Max flux density in stator yoke	1.2 T	1.3 T
16	Max flux density in rotor tooth	1.2 T	1.45 T
17	Gap flux density	0.5 T	0.73 T
18	Weight of copper	3.564 kg	2.494 kg
19	Weight of stator core	4.84 kg	2.262 kg
20	Weight of stator teeth	2.84 kg	2.123 kg
21	Weight of rotor	2.8 kg	1.5 kg

Table 4. Particulars of 6-4-2 configuration of BDFRM.

Sr.	Description	Initial values	Optimized 8-6-4 BDFRM
1	Stator outer diameter	235 mm	210 mm
2	Stator internal diameter (stator bore)	169 mm	144.24 mm
3	Length of air gap (main)	0.45 mm	0.5 mm
4	Rotor external diameter	168 mm	143 mm
5	Effective axial length of machine	106	69 mm
6	Stator yoke length	9 mm	14.5 mm
7	Rotor pole pitch	85.37 mm	75.5 mm
8	Rotor inner diameter	30 mm	35 mm
9	Area of power winding conductor	0.506 mm^2	0.653 sq.mm dia. 0.9118 mm
10	Area of control winding conductor	0.506 mm^2	0.653 sq.mm dia. 0.9118 mm
11	Depth of stator slot	18 mm	26.88 mm
12	Stator tooth width	5 mm	5.1278 mm

Sr.	Description	Initial values	Optimized 8-6-4 BDFRM
13	Slot area	113 mm^2	177.32 sq. mm
14	Total slot space factor	0.45	0.35
15	(ac) Loading of power winding	10 kA/m	12.4 kA/m
16	(ac) Loading of control winding	10 kA/m	9.04 kA/m
17	Max flux density in stator tooth	1.2 T	1.48 T
18	Max flux density in stator yoke	1.2 T	1.48 T
19	Max flux density in rotor tooth	1.2 T	1.38 T
20	Gap flux density	0.5 T	0.5 T
21	Weight of copper	4.559 kg	3.783 kg
22	Weight of stator core	4.989 kg	2.99 kg
23	Weight of stator teeth	3.911 kg	2.86 kg
24	Weight of rotor laminations	7.85 kg	6.8 kg

Table 5. Particulars of 8-6-4 configuration of BDFRM.

b. Power winding poles—8, control winding poles—4, rotor poles(ducted)—6, rated speed 500 rpm, stator slots 48 with two independent windings in stator

A nonlinear optimization technique is based on constrained optimization along with finite element analysis using Maxwell 15 2D software for design optimization of BDFRM. The key dimensions of BDFRM prototypes which are obtained after design optimization are given in **Tables 4** and **5**.

In optimized prototypes of 6-4-2 and 8-6-4 BDFRMs, requirements of active materials have reduced by 50 and 29% respectively. The considerable reduction in active material for 6-4-2 BDFRM is due to the use of single winding in stator. Even though material requirements have gone down, it hardly affects the performance parameters. This can be observed from **Figures 6–8** where the plots for power factor, efficiency, and torque vs. weight of active materials used in

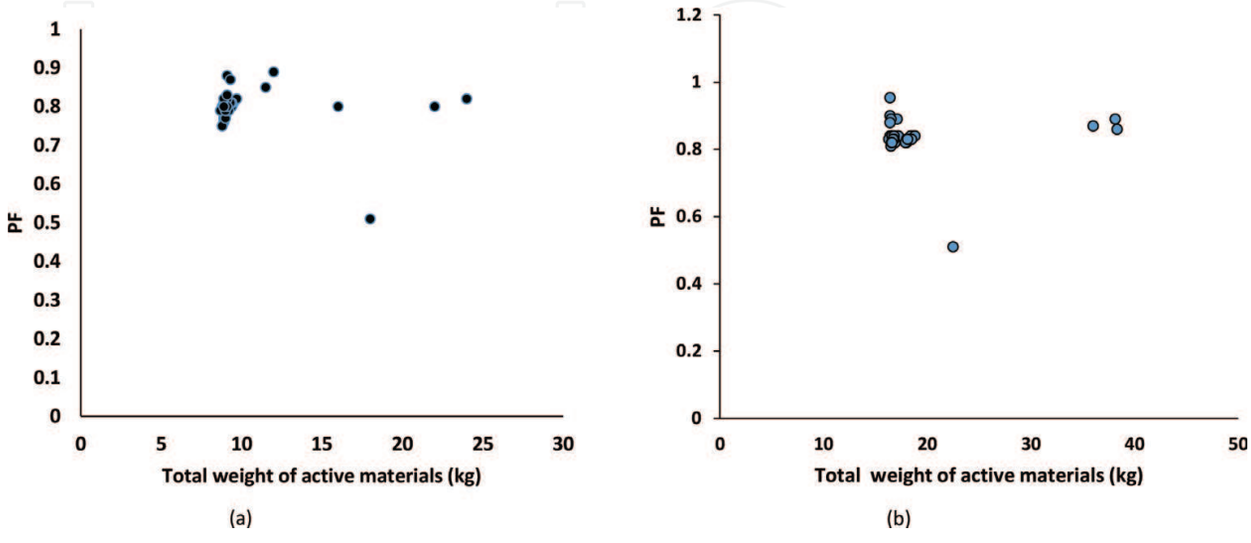

Figure 6. Variation of power factor with weight of active materials. (a) 6-4-2 BDFRM and (b) 8-6-4 BDFRM.

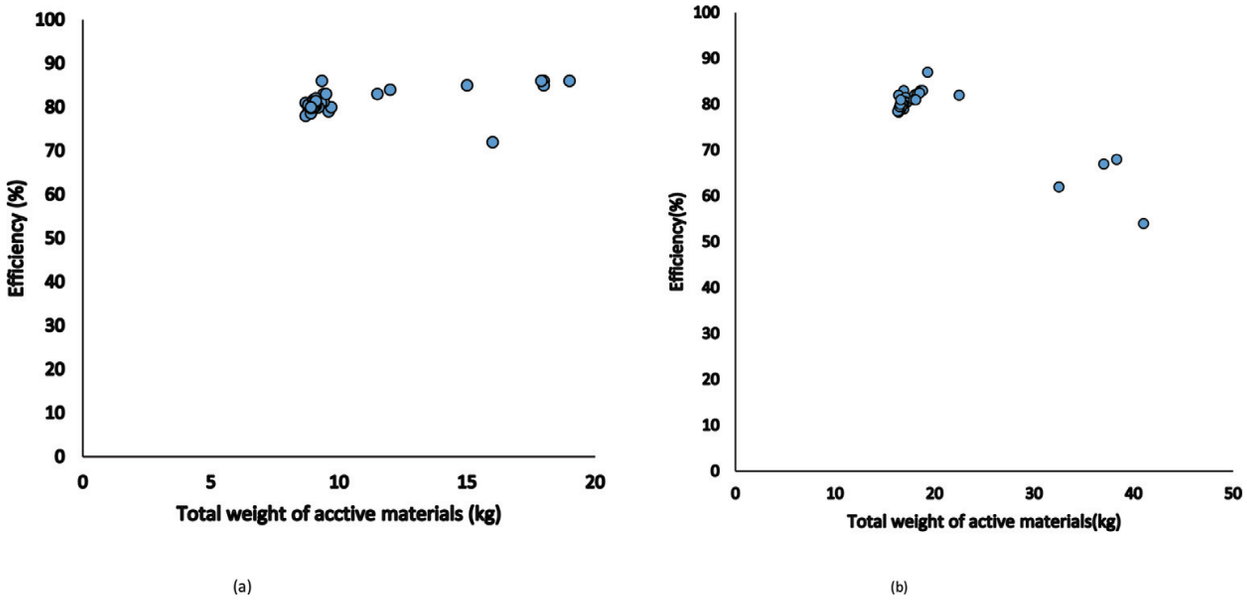

Figure 7. Variation of efficiency with weight of active materials. (a) 6-4-2 BDFRM and (b) 8-6-4 BDFRM.

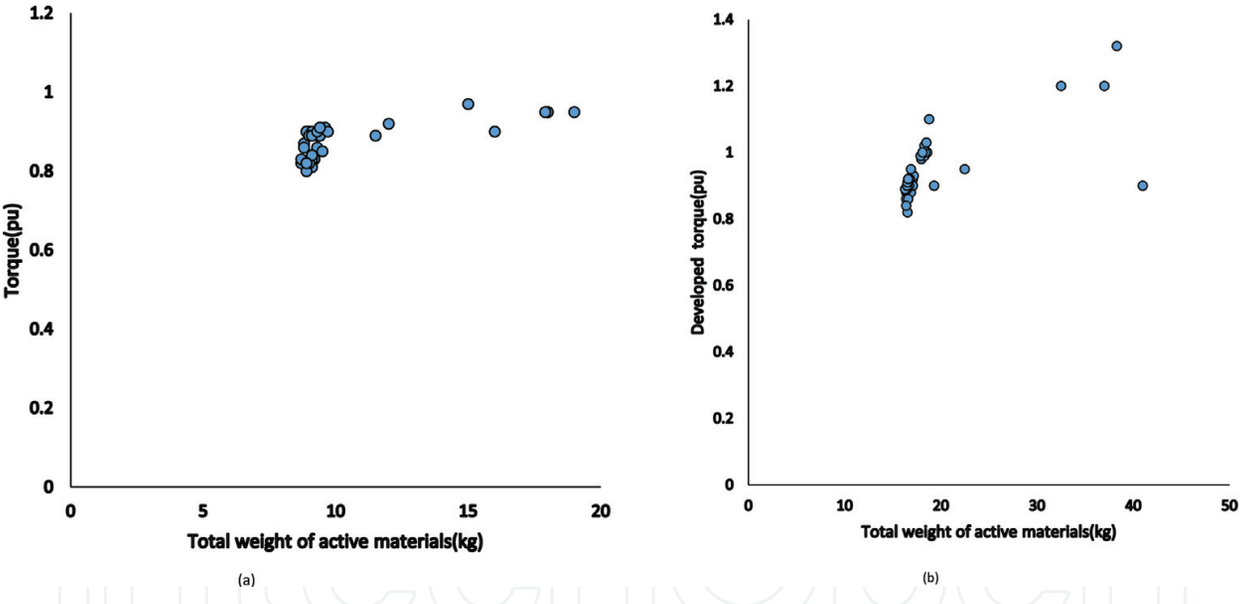

Figure 8. Variation of developed torque (pu) with weight of active materials. (a) 6-4-2 BDFRM and (b) 8-6-4 BDFRM.

BDFRM for all candidate machine designs were evaluated during optimization process, respectively. The data points for these variables form a cluster around the optimum value of active materials.

5. Prototypes of BDFRM

Two prototypes of BDFRM are fabricated based on optimum design, and details of which are given below [21].

http://dx.doi.org/10.5772/intechopen.74805

5.1. 6-4-2 Reluctance rotor configuration

The stator has 36 slots in which a single winding is embedded. The details of stator and rotor laminations (thickness 0.35 mm) used are shown in **Figure 9**.

The details of winding are shown in **Figure 10**. The winding is developed such that two different poles (6 and 2) are formed with single winding. The end connections and coil groups

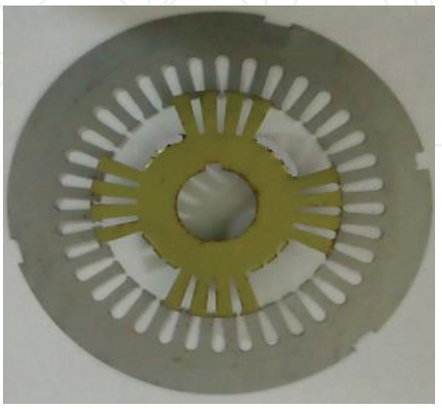

Figure 9. Laminations used in 6-4-2 BDFRM.

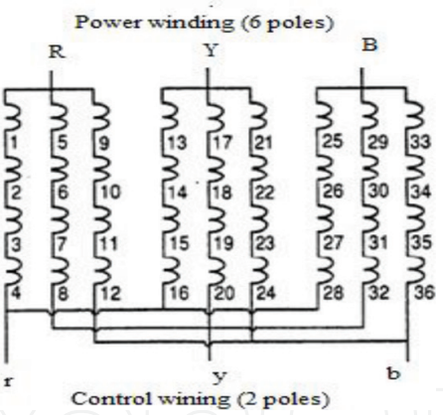

Figure 10. Winding arrangement in 6-4-2 BDFRM.

Figure 11. Fabrication details of 6-4-2 BDFRM.

are connected such that one end behaves as a 6-pole (power) winding and the other end acts as a 2-pole (control) winding. A short-pitched (short pitched by one slot) double-layer winding with 36 coils is designed primarily for two poles. Nine groups are formed with each group having four coils. The start and end terminals of each coil group are brought out for giving flexibility in winding connection. This has resulted in increased length of end connections than the normal case. Hence, special size end covers have to be designed. The actual photographs of 6-4-2 BDFRM during fabrication are shown in **Figure 11**.

5.2. 8-6-4 Circular ducted rotor configuration

8-6-4 Circular ducted rotor BDFRM is fabricated. Stator consists of two independent windings one designed for eight poles (power) and the other for four poles (control). The windings are star connected. The stator windings are accommodated in 48 slots to get full-pitched windings. The lamination has deeper slots so that two double-layer windings can be fitted with a good slot space factor. The use of two double-layer windings facilitated the arrangement of end connections. All terminals of the windings are brought out so as to get flexibility in connection.

The number of ducts per rotor pole is selected as 10 as per the guidelines given in **Table 3** [16, 17]. The fabrication details are shown in **Figure 12**.

Figure 12. Fabrication details of 8-6-4 BDFRM.

6. Finite element analysis of BDFRM

By using MAXWEL 16 software, the finite element models [22] are developed from the actual dimensions of stator and rotor laminations for 6-4-2 and 8-6-4 configurations. The models are simulated to get flux density distribution, torque, and surfaces forces. The flux density distribution in 6-4-2 BDFRM and 8-6-4 BDFRM is shown in **Figure 13(a)** and **(b)**, respectively. It may be observed that flux density values are staying within saturation limit. The peak magnitude of flux density in prototype BDFRMs does not exceed 1.79 T.

http://dx.doi.org/10.5772/intechopen.74805

Reluctance machines develop weak and pulsating torque. BDFRM is not different. This can be seen from **Figure 14(a)**. However, the torque developed by ducted rotor BDFRM is higher with reduced pulsation as shown in **Figure 14(b)**.

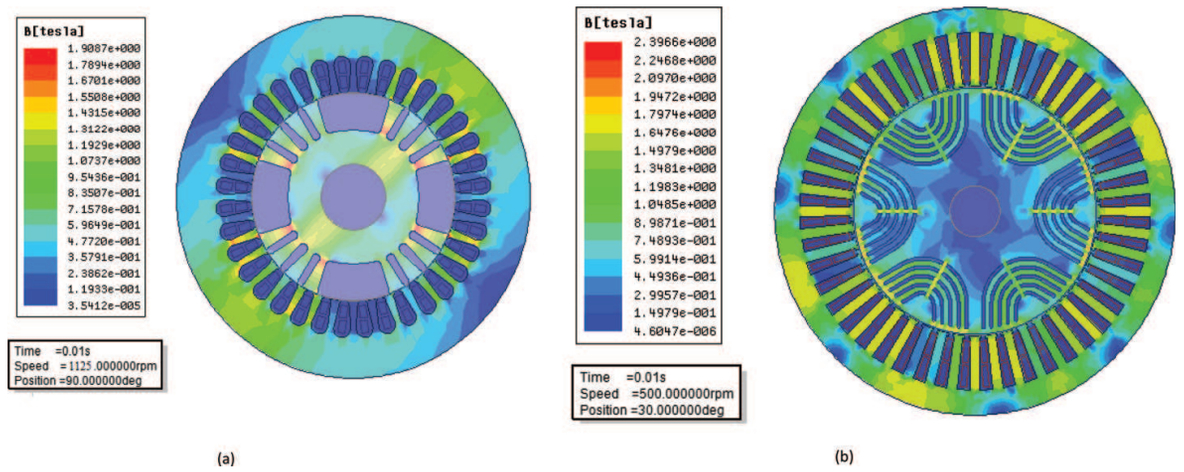

Figure 13. Flux density distribution in BDFRM. (a) 6-4-2 BDFRM and (b) 8-6-4 BDFRM.

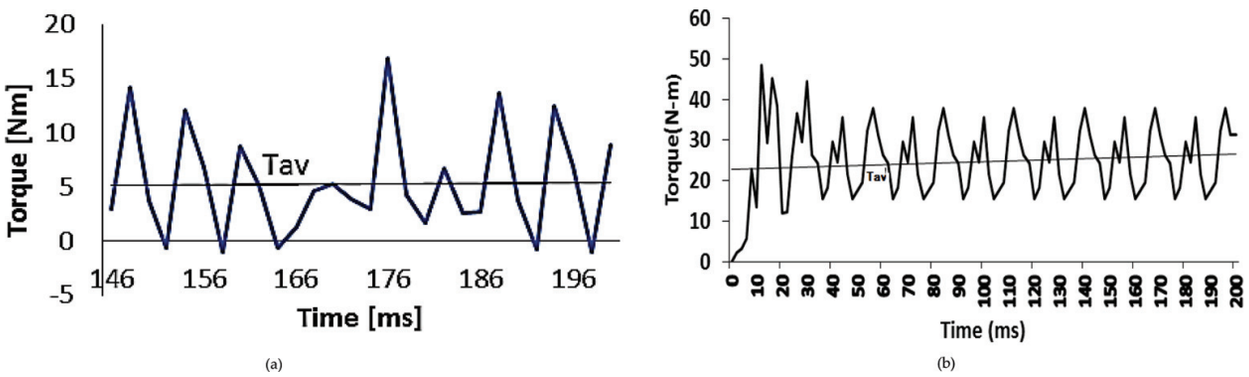

Figure 14. Torque developed by BDFRM. (a) 6-4-2 BDFRM and (b) 8-6-4 BDFRM.

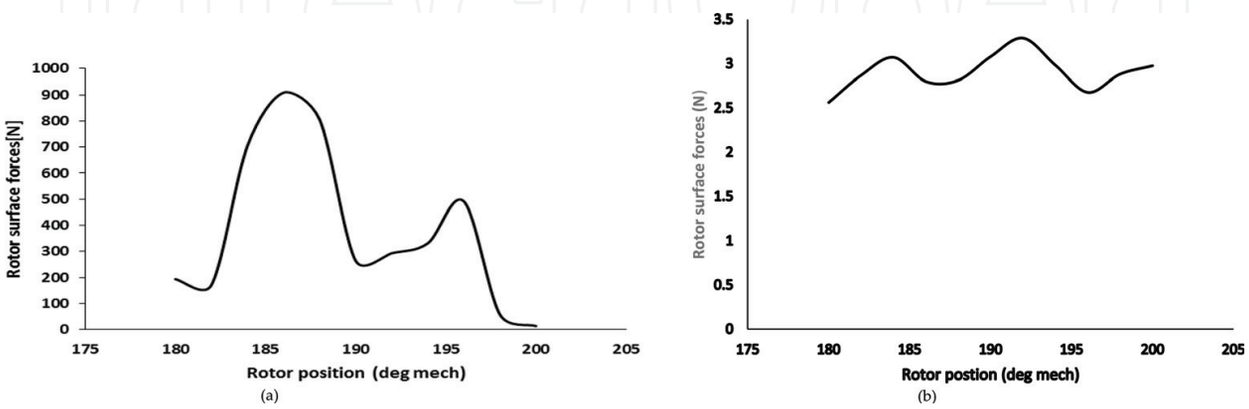

Figure 15. Unbalanced magnetic pull acting on rotor surface. (a) 6-4-2 BDFRM and (b) 8-6-4 BDFRM.

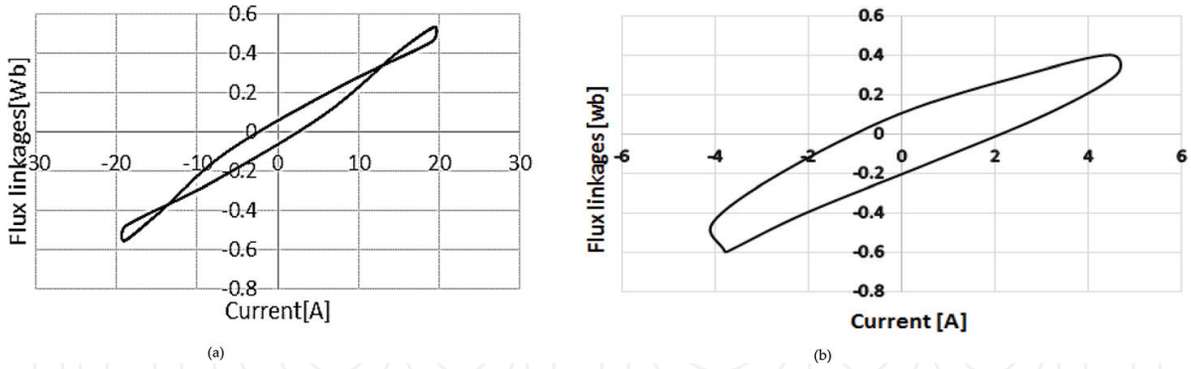

Figure 16. λ-I plots for BDFRM. (a) 6-4-2 BDFRM and (b) 8-6-4 BDFRM.

Due to the absence of winding on rotor in BDFRM, there is no counterbalancing of MMF for stator MMF. This develops unbalanced magnetic forces on rotor surface. The magnitude of forces is quite large in reluctance rotor configuration, whereas they are considerably reduced in case of ducted rotor. This can be seen from **Figure 15**. The magnetic forces greatly reduce with advanced rotor configurations.

The flux linkage-current plots (λ-i) for both configurations are shown in **Figure 16**. The performance of machine greatly depends on area of (λ-i) plot. The plots clearly indicate that 8-6-4 BDFRM has better performance due to larger area of (λ-i) plot.

7. Performance of prototypes

The performances of two prototype BDFRMs are obtained from load tests. BDFRM is coupled with a dc machine of rating 2 kW, 220 V, and 1500 rpm which acts as a load. A three-phase two-level, 3 kW, IGBT variable voltage variable frequency inverter is used for exciting the control

6-4-2 Reluctance rotor BDFRM		Description	8-6-4 Ducted rotor BDFRM	
Optimized machine (calculated)	**Actual value@60% loading**		**Optimized machine (calculated)**	**Actual value@60% loading**
2 kW	1.2 kW	Rated output	2 kW	1.6 kW
750 rpm	750 rpm	Base speed	500 rpm	500 rpm
80%	75%	Efficiency	83%	75%
0.7	0.54	Power factor	0.8	0.7
25.46 N-m	15.27 N-m (from FEA analysis)	Torque developed	38 N	30 N (from FEA analysis)
1.35 T	1.77 T (from FEA analysis)	Flux density in stator tooth	1.48 T	1.77 T (from FEA analysis)
34°C	42°C (by resistance method)	Temperature rise	34.45°C	45°C (by resistance method)

Table 6. Performance details of prototype BDFRMs.

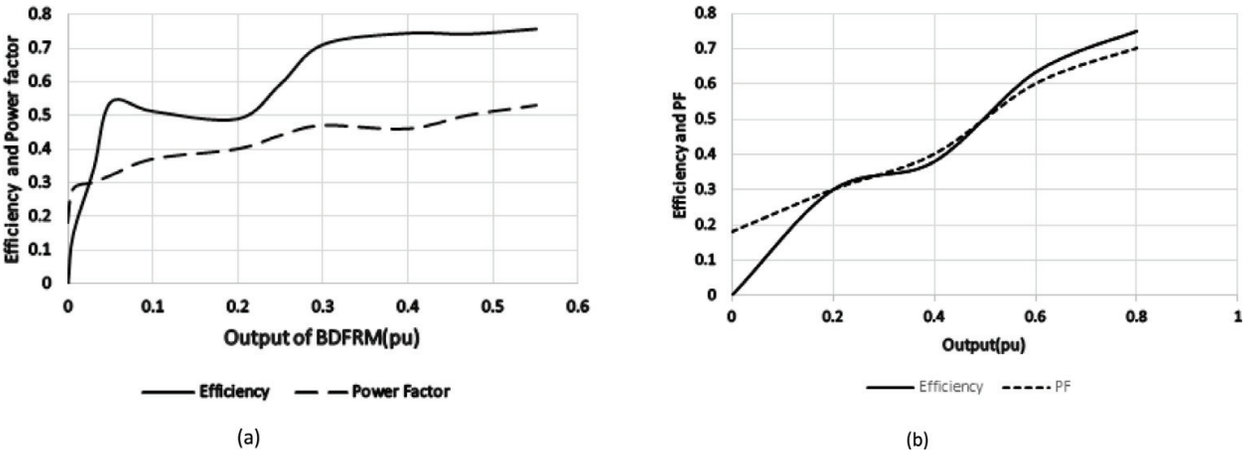

Figure 17. Performance curves of prototype BDFRMS. (a) 6-4-2 BDFRM and (b) 8-6-4 BDFRM.

winding. The results are presented in **Table 6**. Because of the limitation of laboratory test facilities, loading could be done up to 70%.

The capabilities of prototype BDFRMs can be judged from the performance curves shown in **Figure 17**. There is slight deviation of parameters from designed values. This may be due to practical difficulties during loading the machine. Additionally, there is an increase in losses due to the presence of harmonics in control winding excitation which has compromised efficiency and power factor. This advocates development of sophisticated control algorithm for BDFRM to get the desired performance.

8. Conclusion

This chapter highlights various optimization methods, suitability of nonlinear programming methods, and recent stochastic or population-based methods for optimal design of electrical machines. It also discusses briefly a few issues in the design of BDFRM. An objective function is developed for minimization of active material requirement, and an algorithm based on nonlinear programming is presented for optimal design of 2 kW BDFRMs. The analytical models developed based on optimized design are simulated in Maxwell 16 software. The simulation results closely agree with the design values, and there is no saturation in magnetic circuit. The field tests on the two prototypes have demonstrated the capabilities of BDFRMs. It is observed that the performance of 8-6-4 BDFRM is better than 6-4-2 BDFRM in all respects. Both the machines have attained rated speed. Speed control has been achieved on either side of it. Although efficiencies of the prototypes are closer to design values, power factor is lower than expected.

Author details

Mandar Bhawalkar*, Gopalakrishnan Narayan and Yogesh Nerkar

*Address all correspondence to: mandar_bhawalkar@yahoo.co.in

PVG's College of Engineering and Technology, Pune, India

References

[1] Betz R, Jovanovic M. Theoretical analysis of control properties for brushless doubly fed reluctance machine. IEEE Transactions on Energy Conversion. Sept 2002;**17**(1):332-339. DOI: 10.1109/TEC.2002.801997

[2] Betz R, Jovanovic M. The brushless doubly fed reluctance machine and the synchronous reluctance machine—a comparison. IEEE Transactions on Industry Applications. Jul/Aug 2000;**36**(4):1103-1110. DOI: 10.1109/28.855966

[3] Stipetic S, Miebach W, Zarko D. Optimization in design of electrical machines: Methodology and workflow. In: Proceedings of the International Conference on ACEMP-OPTIM-Electromotion Conference; 2015. pp. 441-448

[4] Liu A, Xu W. A global optimization approach for electrical machine designs. IEEE Power & Energy Society General Meeting. 2007:1-8. ISBN: 1-4244-1298-6

[5] Rao S. Engineering Optimization Theory and Practice. 3rd ed. New Delhi: New Age International Publisher; 2013. 722p. ISBN 978-81-224-2723-3

[6] Ramamoorthy M. Computer Aided Design of Electrical Equipments. Reprint. New Delhi: Affiliated East West Press Pvt Ltd; 2011, 2011. pp. 5-53. ISBN 81-85095-57-4

[7] Ma C, Qu L. Multiobjective optimization of switched reluctance motors based on design of experiments and particle swarm optimization. IEEE Transactions on Energy Conversion. Sept. 2015;**30**(3):1144-1153. DOI: 10.1109/TEC.2018.2411677

[8] Jiang W, Jahns T, Lipo T, Taylor W, Suzuki Y. Machine design optimization based on finite element analysis in a high-throughput computing environment. In: Proceedings of IEEE Energy Conversion Congress and Exposition; Sept. 2012. 10.1109/ECCE.2012.6342727

[9] Legranger J, Friedrich G, Vivier S, Mipo J. Combination of finite-element and analytical models in the optimal multidomain design of machines: Application to an interior permanent magnet starter generator. IEEE Transactions on Industry Applications. Jan 2010;**46**(1): 232-239. DOI: 10.1109/TIA.2009.2036549

[10] Ponmurugan P, Rengarajan N. Multiobjective optimization of electrical machines, a state of the art study. Journal of Computer Applications. Oct. 2012;**56**(13):26-30. DOI: 10.1.1.244.6959

[11] Idir K, Chang L, Dai H. A neural network based optimization approach for induction motor design. Canadian Conference on Electrical & Computer Engineering; May1996. pp. 951-954

[12] Bétin F, Yazidi A, Sivert A, Fuzzy CG. DOI n DOI logic control design for electrical machines. International Journal of Electrical Engineering and Technology. May–June 2016; **7**:14-24. ISSN 0976-6545

[13] Çuncaş M. Design optimization of electric motors by multiobjective fuzzy genetic algorithm. Mathematical and Computational Applications. 2008;**13**(3):153-163

[14] Liao Y, Xu L, Li Z. Design of a doubly fed reluctance motor for adjustable speed drive. IEEE Transactions on Industry Applications. Sept/Oct 1996;**32**(5):1195-1203. DOI: 10.1109/28.536883

[15] Knight A, Betz R, Dorrell D. Issues with the design of brushless doubly fed reluctance machines: Unbalanced magnetic pull, skew and iron losses. 2011 IEEE International Electric Machines & Drives Conference (IEMDC); 2011. pp. 663-668

[16] Knight A, Betz R, Dorrell D. Design and analysis of brushless doubly fed reluctance machines. IEEE Transactions on Industry Applications. Jan/Feb 2013;**49**:50-57. DOI: 10.1109/TIA.2012.2229451

[17] Vagati A, Franceschini G, Marongiu I, Troglia G. Design criteria of high performance synchronous reluctance motors. IAS Annual Meeting. 1992;**1**:66-73

[18] Vagati A, Pastorelli M, Francheschini G, Petrache S. Deign of low torque ripple synchronous reluctance motor. IEEE Transactions on Industry Applications. 1998;**34**(4):758-765. DOI: 10.1109/IAS.1997.643040

[19] Boldea I. Reluctance Synchronous Machines and Drives. New York, USA: Oxford Science Publications; 1996. ISBN: 0 19 85391 0

[20] Kunte S, Bhawalkar M, Gopalakrishnan N, Nerkar Y. Optimal design and comparative analysis of different configurations of brushless doubly fed reluctance machine. IEEJ Transactions on Industry Applications. Nov. 2017;**6**(6):370-380. DOI: 10.1541/ieejjia.6.370

[21] Bhawalkar M. Studies in Wind Power Generation Systems [Ph.D. Thesis]. India: Savitribai Phule Pune Univeristy; Oct. 2017

[22] Bianchi N. Electrical Machine Analysis Using Finite Elements. FL, USA: Taylor and Francis, Special Indian reprints; 2015. ISBN 9780849333996

IntechOpen